AFRL-RX-WP-TP-2011-4233

ACCUMULATION OF TIME-DEPENDENT STRAIN DURING DWELL-FATIGUE EXPERIMENTS OF iBN-SYLRAMIC MELT INFILTRATED SiC/SiC COMPOSITES WITH AND WITHOUT HOLES (PREPRINT)

R. John

Metals Branch
Metals, Ceramics, and NDE Division

G. Ojard and R. Miller

Pratt & Whitney

Y. Gowayed and J. Chen

Auburn University

G. Morscher

Ohio Aerospace Institute

U. Santhosh and J. Ahmad

Research Applications, Inc.

JULY 2011

AIR FORCE RESEARCH LABORATORY
MATERIALS AND MANUFACTURING DIRECTORATE
WRIGHT-PATTERSON AIR FORCE BASE, OH 45433-7750
AIR FORCE MATERIEL COMMAND
UNITED STATES AIR FORCE

REPORT DOCUMENTATION PAGE

Form Approved
OMB No. 0704-0188

1. REPORT DATE *(DD-MM-YY)*	2. REPORT TYPE	3. DATES COVERED *(From - To)*
July 2011	Journal Article Preprint	01 July 2011 – 01 July 2011

4. TITLE AND SUBTITLE

ACCUMULATION OF TIME-DEPENDENT STRAIN DURING DWELL-FATIGUE EXPERIMENTS OF iBN-SYLRAMIC MELT INFILTRATED SiC/SiC COMPOSITES WITH AND WITHOUT HOLES (PREPRINT)

5a. CONTRACT NUMBER
In-house

5b. GRANT NUMBER

5c. PROGRAM ELEMENT NUMBER
62102F

6. AUTHOR(S)

R. John (AFRL/RXLM)
G. Ojard and R. Miller (Pratt & Whitney)
Y. Gowayed and J. Chen (Auburn University)
G. Morscher (Ohio Aerospace Institute)
Unni Santhosh and Jalees Ahmad (Research Applications, Inc.)

5d. PROJECT NUMBER
4347

5e. TASK NUMBER
20

5f. WORK UNIT NUMBER
LN101100

7. PERFORMING ORGANIZATION NAME(S) AND ADDRESS(ES)

Metals Branch (AFRL/RXLM)
Metals, Ceramics, and NDE Division
Air Force Research Laboratory, Materials and Manufacturing Directorate
Wright-Patterson Air Force Base, OH 45433-7750
Air Force Materiel Command, United States Air Force

Pratt & Whitney
East Hartford, CT

Auburn University
Auburn, AL

Ohio Aerospace Institute
Cleveland, OH

Research Applications, Inc.
11772 Sorrento Valley Road, Suite 260
San Diego, CA 92121-1085

8. PERFORMING ORGANIZATION REPORT NUMBER
AFRL-RX-WP-TP-2011-4233

9. SPONSORING/MONITORING AGENCY NAME(S) AND ADDRESS(ES)

Air Force Research Laboratory
Materials and Manufacturing Directorate
Wright-Patterson Air Force Base, OH 45433-7750
Air Force Materiel Command
United States Air Force

10. SPONSORING/MONITORING AGENCY ACRONYM(S)
AFRL/RXLM

11. SPONSORING/MONITORING AGENCY REPORT NUMBER(S)
AFRL-RX-WP-TP-2011-4233

12. DISTRIBUTION/AVAILABILITY STATEMENT
Approved for public release; distribution unlimited.

13. SUPPLEMENTARY NOTES
PAO Case Number: 88ABW 2010-3642; Clearance Date: 02 Jul 2010. Document contains color.
Journal article submitted to the *Journal: Composites Science & Technology*.

14. ABSTRACT

Accumulation of time-dependent strain during dwell-fatigue experiments of iBN-Sylramic Melt Infiltrated SiC/SiC composites is investigated. A 2-hour load cycle is repeated for specimens without holes and specimens with a central hole under the following conditions: i) a stress ratio of 0.05, ii) various stress levels, iii) 815 °C and 1204 °C, iv) different times up to 600 hours, and v) different hole diameters. An increase in the accumulation of time-dependent strain with the increase in time and stress level is observed for specimens with and without holes with the time-dependent strain at 1204 °C, much higher than that observed at 815 °C. All specimens recovered part of their time-dependent strain at the minimum stress level and the value of both time-dependent strain and recovery strain depreciated with time.

15. SUBJECT TERMS
ceramic matrix composites (CMCs), modeling, time-dependent response, dwell fatigue

16. SECURITY CLASSIFICATION OF:			17. LIMITATION OF ABSTRACT:	18. NUMBER OF PAGES	19a. NAME OF RESPONSIBLE PERSON (Monitor)
a. REPORT	b. ABSTRACT	c. THIS PAGE			Reji John
Unclassified	Unclassified	Unclassified	SAR	30	19b. TELEPHONE NUMBER *(Include Area Code)* N/A

Accumulation of time-dependent strain during dwell-fatigue experiments of iBN-Sylramic Melt Infiltrated SiC/SiC composites with and without holes

G. Ojard[2], Y. Gowayed[3], J. Chen[3], G. Morscher[4], R. Miller[2], U. Santhosh[5], J. Ahmad[5] and R. John[1]

[1] Air Force Research Laboratory, AFRL/RXLM, Wright-Patterson AFB, OH
[2] Pratt & Whitney, East Hartford, CT
[3] Auburn University, Auburn, AL
[4] Ohio Aerospace Institute, Cleveland, OH
[5] Research Applications, Inc., San Diego, CA

Abstract

Accumulation of time-dependent strain during dwell-fatigue experiments of iBN-Sylramic Melt Infiltrated SiC/SiC composites is investigated. A two-hour load cycle is repeated for specimens without holes and specimens with a central hole under the following conditions: i) a stress ratio of 0.05, ii) various stress levels, iii) 815 ^{o}C and 1204 ^{o}C, iv) different times up to 600 hours and v) different hole diameters. An increase in the accumulation of time-dependent strain with the increase in time and stress level is observed for specimens with and without holes with the time-dependent strain at 1204 ^{o}C much higher than that observed at 815 ^{o}C. All specimens recovered part of their time-dependent strain at the minimum stress level and the value of both time-dependent strain and recovery strain depreciated with time.

Residual strain to failure for specimens without holes that did not fail during dwell fatigue experiments showed a reduction with the increase in the amount of strain accumulated during the experiment. A curve fitting procedure of this experimental data, as well as data from archived literature, pointed at the possibility of the existence of a finite amount of strain to failure of all specimens tested at both temperatures. This was observed regardless of the value of the stress or the strain rate, as long as the maximum stress was below a certain critical value close to the end of the knee of the stress-strain curve.

Accumulation of time-dependent strain in the vicinity of a central hole is studied using Finite Element Analysis utilizing data from experiments without holes. A large increase in strain accumulation with time is observed in the vicinity of the hole, up to 9 times higher than strain in areas far from the hole.

Key words: Ceramic Matrix Composites (CMCs), Modeling, time-dependent response, Dwell fatigue.

Introduction

As Ceramic Matrix Composites (CMCs) are being considered for long duration applications, a strong understanding of their behavior under conditions of sustained load at operating temperatures is needed. Examples of long term applications can be found in ground base turbines for power generation where CMCs are being considered for combustor liners, turbine vanes and shroud applications [1,2]. These applications can experience operational times in

excess of 30,000 hours (> 3 years) with various loading and unloading scenarios. Such long term applications leverage the high temperature material capability while taking advantage of the weight reduction, reduced cooling and durability improvements that CMCs can provide.

It can be envisaged that any CMC used as a combustor liner or as a vane will need to be attached to another material to be held in place, even if there is only a need for a location pin or a way to stop rotation; a feature that breaks the continuity of the reinforcing fibers and requires some machining. Hence, it is imperative that our understanding of their behavior should include the effect of the existence of a feature such as a through-thickness hole.

The material under investigation in this study is iBN Melt Infiltrated (MI) SiC/SiC CMC developed under the Enabling Propulsion Materials Program and labeled N24. To manufacture MI SiC/SiC composites, Sylramic® fiber tows, with 800 fibers per tow, are woven into 5-harness satin balanced weaves with 20 ends per inch. An in-situ Boron Nitride (iBN) treatment is applied to these weaves forming a fine layer of BN on the surface of every fiber. Eight layers of the fabric are laid in a graphite mold, with holes allowing gas infiltration, and a BN coat is applied to the fibers via a Chemical Vapor Infiltration (CVI) process to further protect the surface of the fibers. SiC is introduced to the coated layers via a CVI process up to around 30% volume ratio of open porosity of the panel. SiC particulates are then slurry cast into the panel followed by melt infiltration of a Si alloy. The panel at this time typically has around 2% volume ratio of open porosity. Manufacturing details of this composite, micrographs of its internal structure and its mechanical properties at room temperature and 1204 ^{o}C can be found elsewhere [3,4].

In this article, we attempt to add to the knowledge of the time-dependent response of this material to aid in its design for long term applications. We present a study of the accumulation of time dependent strain during dwell fatigue experiments conducted on specimens with and without a central hole. The impact of the existence of the hole as well as the size of the hole are delineated and a numerical technique is used to shed light on the distribution of accumulated time-dependent strain around the hole. Two temperatures are investigated, 1204 ^{o}C as the main projected operating temperature and 815 ^{o}C as a possible temperature where pesting may take place in SiC/SiC composites [5]. Residual strength experiments for specimens that did not fail during dwell fatigue tests are reported and analyzed to understand the effect of the environmental exposure at the testing temperature and the accumulation of the time-dependent strain on the material.

Experimental procedures

Specimens without holes were 165.1 mm long and 12.7 mm wide with a reduced gage section of 27.5 mm long by 8.255 mm wide. The transition radius into the gage section was set at 307.34 mm. Specimens with holes were 152.4 mm long, without a reduced gage section, with a central hole-diameter of 2.286, 4.572 or 6.35 mm located at the center of the gage length. The width of the specimens with the central hole was 5 times the diameter of the hole. All specimens had an average thickness of 2.1 mm.

Tensile testing was conducted on specimens at 24 ^{o}C, 815 ^{o}C and 1204 ^{o}C to characterize the material instantaneous behavior under different stress levels at these temperatures as shown in Figure 1. Similar tests were conducted for specimens with holes at 1204 ^{o}C as shown in Figure 2.

All dwell-fatigue experiments were conducted in air using a SiC furnace at 1204 ^{o}C or 815 ^{o}C with the temperature controlled by using a thermocouple placed on the specimen. Load was cycled on and off every two hours at a strain rate of 1.24×10^{-4} s^{-1} for load-up and unload. A typical load-time profile is shown in Figure 3 which was adopted to mimic possible operational conditions. Load was applied using a dead weight with a lever arm that is controlled by a cam system. Strain was recorded using a single 25.4 mm extensometer for the entire test. Experiments were conducted at various times up to 600 hours.

Specimens without holes tested at 1204 ^{o}C were subjected to stress levels of 110.4, 165.6, 193.2 and 220.8 MPa at a stress ratio of 0.05 with at least three specimens per data point. At 815 ^{o}C, specimens were only subjected to stress levels of 110.4, 165.6 MPa to check for pesting conditions with at least two specimens per data point. The number of specimens was determined based on the availability of the material. The stress of 110.4 MPa was selected because it is in the linear elastic region of the tensile stress-strain curve while stresses 165.6 and 193.2 MPa are within the knee region where in-elastic strain is occurring indicating that the matrix is cracking allowing for some environmental attack into the specimens. Stress 220.8 MPa was selected to show the material behavior at the end of the knee region at a point of possible matrix crack saturation [6].

Specimens with holes were only tested at 1204 ^{o}C. Specimens with a 2.286 mm central hole were subjected to net section stress levels of 55.16, 110.4, 165.6 and 193.2 MPa to evaluate the effect of the existence of a hole on the strain response. Specimens with 4.572 and 6.35 mm central holes were tested at 55.16 and 110.4 MPa to evaluate the effect of the hole size. Stress 55.16 MPa was selected to show the specimen response at a low stress level in the linear region of the tensile stress-strain curve, and 110.4, 165.6 and 193.2 MPa net-section stresses were chosen to allow for comparison with specimens without holes. Two specimens, per data point, were tested at 55.16 and 110.4 MPa for all central hole-diameters, and one specimen per data point, was tested at 165.6 and 193.2 MPa for the 2.286 mm hole. The number of specimens was determined based on the availability of the material.

Residual strength experiments were conducted for specimens without holes and specimens with 2.286 and 4.572 mm central holes that did not fail in dwell fatigue experiment. Specimens without holes tested in dwell fatigue at 1204 ^{o}C, were tested for their residual strength at room temperature and 1204 ^{o}C, while specimens tested in dwell fatigue at 815 ^{o}C were tested at room temperature and 815 ^{o}C. Experiments were carried out by loading the specimens in tension until failure at a strain rate of 1.59×10^{-4} s^{-1}.

Analysis of experimental results

A Matlab® code was developed to extract the time-dependent strain for each cycle out of the large amount of data acquired during these experiments. Using this tool, a typical stress-strain response for the first few cycles in the dwell fatigue experiments can be represented as shown in Figure 4. For all specimens, each load cycle followed a hysteresis loop. As the specimen is loaded, a strain response, similar to that of the tensile stress-strain curve, is observed. During the two hour at the hold stress, time-dependent strain accumulates, and upon unload the specimen recovers part of its accumulated strain. At the minimum stress level, the specimen recovers an additional part of its accumulated strain. The area of the hysteresis loop of the first cycle was much larger than that observed in subsequent cycles and continued to decrease with additional cycles.

Specimens without holes: Figure 5 shows the total (elastic + time-dependent) strain versus time for specimens without holes tested at 1204 ^{o}C under 110.4, 165.6, 193.2 and 220.8 MPa stress levels. The elastic component of the strain increased linearly with the increase in the stress and the rate of accumulation of time-dependent strain increased with the increase in the stress level. Three tests were conducted at 220.8 MPa, which is at the end of the knee in the stress-strain curve as shown in Figure 1, with two of the specimens failing in less than two hours and the third specimen surviving for 250 hours without failure pointing at the possibility that this stress level is at the edge of the material capability. The mathematical function for the increase in the accumulation of the time-dependent component was extracted from data fitting using a 3-parameter curve fitting approach, indicated on Figure 5 by solid lines, according to the equation:

$$Time\ dependent\ strain\ = A\sigma^{n}t^{p} \qquad \ldots(1)$$

Where, A=1.5x10^{-23}, n=2.31, p=0.33, σ = applied stress in Pascals, and t = time in hours. A reasonable level of consistency between the curve fit and the data can be observed.

Figure 6 shows that specimens tested at 815 ^{o}C exhibited an increase in the total strain with the increase in the stress level but the accumulation of the time-dependent strain was less than that observed at 1204 ^{o}C. Curve fitting using Equation (1) was reasonably successful as seen from Figure 6. It yielded similar values for constants n and p but a different value for constant A (A=0.2x10^{-23}). Other than the two specimens that failed at 220.8 MPa mentioned above, no other specimens without holes failed at either temperature.

It was observed that time-dependent strain accumulation at the maximum stress during hold time and strain recovery, measured as the strain recovered at the minimum stress, are not constant from cycle to cycle. Figure 7 shows the change in the value of these time-dependent strains over time for specimens loaded at stresses of 110.4 and 165.6 MPa. A 2-parameter curve fitting equation was used to evaluate that change:

$$Time\ dependent\ strain\ per\ hour = mt^{b} \qquad \ldots(2)$$

Where, *m* and *b* are constants and t is time in hours. The value of m at the 110.4 MPa stress was $4x10^{-5}$ for strain accumulation $4.34x10^{-5}$ for strain recovery and at the 165.6 MPa stress was $1.22x10^{-4}$ for strain accumulation and $1.30x10^{-4}$ for strain recovery. The value of the constant *b* at 110.4 MPa stress for strain accumulation was -0.152 and for strain recovery was -0.212, while its value at 165.6 MPa stress for strain accumulation was -0.192 and for strain recovery was -0.251.

Specimens with a central hole: Figures 8 to 10 show the change of the total apparent strain with time for specimens with a central hole. The term "apparent strain" is used because the hole is located in the middle of the gage section hindering the ability to directly compare its value to the value of the strain for specimens without holes shown in Figure 5. It can be seen that the value of the total apparent time-dependent strain consistently increased with the increase in the net-section stress level and the increase of the time of exposure at load. Only one specimen with a 2.286 mm central hole tested at 193.2 MPa and shown in Figure 6 failed after 34 hours. It can be seen by comparing data in Figures 8 to those in Figure 5, that except for the failed specimen, the pattern of strain accumulation for specimens with a central hole is similar to those without it.

Residual strength: Tensile testing was conducted on specimens that did not fail during dwell-fatigue experiments. For specimens without holes tested in tension at room temperature, a reduction of strength was evident with the passage of time. Also, the higher the stress endured during dwell fatigue experiments, the lower the stress needed to fail the specimen. Specimen loaded at 220.8 MPa in dwell fatigue showed the largest reduction in strength with time of exposure. This is expected due of the high density of cracks at this stress level.

Figure 11 shows a plot of the strain to failure during residual strength experiments for specimens without holes versus time-dependent strain accumulated during dwell fatigue experiment tested at both temperatures. It can be seen that, regardless of temperature for the dwell fatigue test or the residual strength test, as the time-dependent strain accumulation increases, the residual strain to failure decreases. Figure 11 also includes data reported in [7] from the same material for samples tested in residual strength after creep testing and samples that failed during creep. Curve fitting using a linear operator for all of these samples yielded the equation:

$$\text{Residual strain} = -0.952 \times \text{strain evolved during test} + 0.0048 \qquad \ldots(3)$$

The effect of the net-section stress level and time duration on the strength of specimens with holes was not as evident or consistent as they were for specimens without holes. The effect of the diameter of the hole was negligible which can be attributed to the constant ratio of the hole-diameter to specimen width adopted in these experiments.

Finite Element Analysis

It is mathematically infeasible to compare time-dependent strain for specimens without holes to apparent time-dependent strain for specimens with a central hole in which the hole is situated inside the gage region. Additionally, it is hard to experimentally evaluate the time-dependent strain accumulation in the immediate vicinity of the hole. In order to shed light on these two issues a Finite Element analysis was carried out using ANSYS® software.

A specimen with a central hole was constructed in ANSYS® and meshed using element type PLANE 182 to map the model in 2D and element type SOLID185 was used to run the analysis in 3D. A fine mesh was defined around the hole as shown in Figure 12. The orthotropic time-dependent behavior of the material was represented by a combination of Hill's anisotropy model and the implicit Creep Model 6 in ANSYS® utilizing equation (1).

Values of time-dependent strain accumulation at four different locations around the hole for samples tested at 1204 ^{o}C are shown in Figure 13. Location 1 is where the extensometer leg was placed 1.27 cm above the center of the hole at the edge of the specimen, point 2 is located 1.27 cm above the hole at the center of the specimen, point 3 is at the center between the edge of the hole and the edge of the specimen and point 4 is at the edge of the hole. Figure 13 shows the model output for a 4.572 mm central hole loaded at 55.16 MPa, as an example. It can be seen that the local time-dependent strain accumulation at the edge of the hole is much higher than that at any other location. In this specific case, the time-dependent strain accumulation at the hole edge (point 4) was estimated to be as high as 9 times higher in value than that reported by the extensometer (located at point 1) after 250 hours and continued to increase with time.

Model runs were verified by comparing their results to data acquired at point 1 for different hole-diameters at different stress levels as shown in Figure 14. Strain accumulations over time calculated by the model were lower than those acquired at 55.16 MPa and reasonably close to those acquired at 110.4 MPa. Similar results were observed for other hole sizes.

Discussion and conclusions

Dwell fatigue experiments were conducted on MI SiC/SiC composites to study the effect of repeated load/unload on specimens with and without holes at 815 ^{o}C or 1204 ^{o}C and a stress ratio of 0.05. A multitude of stress levels and hole-diameters, with the ratio of hole-diameter to specimen width maintained at 20%, were investigated. Based on the results presented above, the following discussion items and conclusions can be stated:

1. Data for time-dependent strain for specimens without holes showed a relatively consistent increase of strain accumulation with time and stress level. Curve fitting using a 3-parameter curve was reasonably successful for 1204 and 815 ^{o}C as shown in Figures 5 and 6. Constants used for curve fitting listed in Equation (1) were similar at both temperatures except for the constant (A) which was much lower at 815 ^{o}C than at 1204 ^{o}C leading to the conclusion that

time-dependent strain at the former temperature is lower than that at the latter and that pesting as observed in [8] was not witnessed at 815 ^{o}C.

2. Time dependent strain accumulation was observed at the maximum stress level. This can be caused by crack opening and creep of the Si alloy. With the cracks open, the surrounding environment ingresses into the composite, causes oxidation of the BN coat, produces a glassy phase [5,9] that bonds fibers and matrix in the region of the matrix crack and seals the crack. Unloading and loading the specimen breaks the seal and allow further ingress of the environment. Images taken of the failure region after residual strength tests revealed the existence of a glassy phase formed around fibers as shown in Figure 15 for specimen tested in dwell fatigue at a stress of 220 MPa.

3. A considerable amount of the strain accumulated at the maximum stress level was recovered at the minimum stress as shown in Figure 4. A similar phenomenon was witnessed by Reynauld et al for a CVI SiC/SiC composite [10]. Both strains decayed with time as shown in Figure 7 and an empirical equation was obtained for such decay using a 2-parameter curve fit. Strain recovery can be caused by a partial closure of the matrix cracks upon unload, or an elastic rebound, or both. If it is due to crack closure, then the decay in the recovery strain can be caused by the production of the glassy phase within the crack limiting its closure motion. It should be noted that at a stress of 193.2 MPa the average matrix crack spacing was reported to be greater than 2 mm and that the matrix cracks are not through-the-thickness [7]. The proposed deformation mechanism is possible at such high crack density. If the strain recovery is due to an elastic rebound, its reduction over time can be explained by the buildup of the time-dependent strain in the matrix and its resistance to elastic recovery.

4. Specimens with a central hole-diameter of 2.286, 4.572 or 6.35 mm showed an increase in strain accumulation with time as shown in Figures 8-10. Since it is not possible to evaluate the effect of the existence of a hole by directly comparing the value of apparent strain of specimens with a central hole to the value of the strain for specimens without a hole a numerical analysis was conducted using ANSYS®. The numerical model showed a marked increase in the value of strain accumulation in the vicinity of the hole, as shown in Figure 13. This can cause cracks at the sides of the holes allowing the oxidizing environment to ingress into the specimen causing a reduction in the strength of the specimen over time. Contrary to this conclusion, such reduction in strength was not evident from experimental data. It is hypothesized that the applied maximum stress level was not high enough for large cracks to form and impact the strength of the specimens.

   The numerical analysis was also used to calculate the value of the time-dependent strain accumulation at a point where the leg of the extensometer was located for specimens with a central hole as shown in Figure 14. The calculated values were close to values obtained for specimens without holes showing that, for the test duration, the impact of the hole on

strain distribution is limited to the area around the hole and does not affect the overall time-dependent strain accumulation in the far field region.

5. Residual strength experiments for specimens without holes showed a reduction in strength after dwell fatigue experiments. This was particularly true for specimens loaded at a stress level close to the end of the knee of the stress strain curve due to possible crack saturation at such high stress level. A reduction in the strength with the passage of time spent during dwell fatigue experiments was also noticed for most specimens.

6. Residual strain to failure showed a reduction with the increase in accumulated time-dependent strain during dwell fatigue experiments as shown in Figure 11. Curve fitting using Equation (3) showed a reasonable agreement with data for specimens without holes regardless of the stress level or the time of exposure. It seems that the amount of the total strain to failure for all of these specimens is similar. A possible explanation to this observation can be that the strain to failure is mainly controlled by the iBN-Sylramic fibers which are less prone to time-dependent strain [10] than any other constituent in the composite. Following this logic, the time to failure, within a dwell fatigue experiment, can be estimated using Equations (1) and (3) for specimens under different stress levels and strain rates. Specimens with holes, similar to the ones used in this study, are expected to have a much shorter time to failure.

Acknowledgement
The Air Force Research Laboratory, Materials & Manufacturing Directorate, Wright-Patterson AFB, OH, USA supported this effort under contracts F33615-01-C-5234 and F33615-03-D-2354-D04.

References

1. Brewer D., Ojard G. and Gibler M. Ceramic Matrix Composite Combustor Liner Rig Test. ASME Turbo Expo, Munich, Germany (2000); ASME Paper No. 2000-GT-0670.
2. Calomino A, and Verrilli M. Ceramic Matrix Composite Vane Sub-element Fabrication. ASME Turbo Expo, Vienna, Austria (2004); ASME Paper No. 2004-53974.
3. Yun HM, Gyekenyesi JZ, Chen YL, Wheeler DR, and DiCarlo JA. Tensile Behavior of SiC/SiC Composites Reinforced By Treated Sylramic SiC Fibers. Cer. Eng. Sci. Proc. (2001);22(3): 521-531.
4. Gowayed, Y., Ojard, G., Miller, R., Santhosh, U., Ahmad, J., John, R.“ Correlation of elastic properties of melt infiltrated SiC/SiC composites to in situ properties of constituent phases”, Composites Science and Technology 70 (2010) 435–441.
5. Ogbuji L. A Pervasive Mode of Oxidative Degradation in a SiC–SiC Composite. J. Am. Ceram. Soc. (1998);81(11):2777–2784.
6. Ojard, G., Gowayed, Y., Morscher, G., Santhosh, U., Ahmad, J., Miller, R. and John, R., “Creep And Fatigue Behavior of MI SiC/SiC Composites at Temperature”, submitted to Ceramic Engineering and Science Proceedings, 2009.
7. Morscher, G., Ojard, G., Miller, R., Gowayed, Y., Santhosh, U., Ahmad, J., and John, R., “Tensile creep and fatigue of Sylramic-iBN melt-infiltrated SiC matrix composites: Retained properties, damage development, and failure mechanisms,” Composites Science and Technology 68 (2008) 3305–3313.
8. Ogbuji, L., “Degradation of a SiC/SiC composite in the burner rig: investigation by fractography, Materials at high temperatures 17(2) 369–372 (2000)
9. Morscher G, Hurst J, and Brewer D. Intermediate-Temperature Stress Rupture of a Woven Hi-Nicalon, BN-Interphase, SiC-Matrix Composite in Air. J. Am. Ceram. Soc. (2000);83(6): 1441–1449.
10. Reynaud, P., Rouby, D. and Fantozzi, G., “Effects of temperature and of oxidation on the interfacial shear stress between fibres and matrix in ceramic-matrix composites”, Acta mater., vol 46, No. 7, pp 2461-2469, 1998.
11. Yun HM, and DiCarlo JA. Comparison of the Tensile, Creep, and Rupture Strength Properties of Stoichiometric SiC Fibers. NASA/TM – 1999-209284.

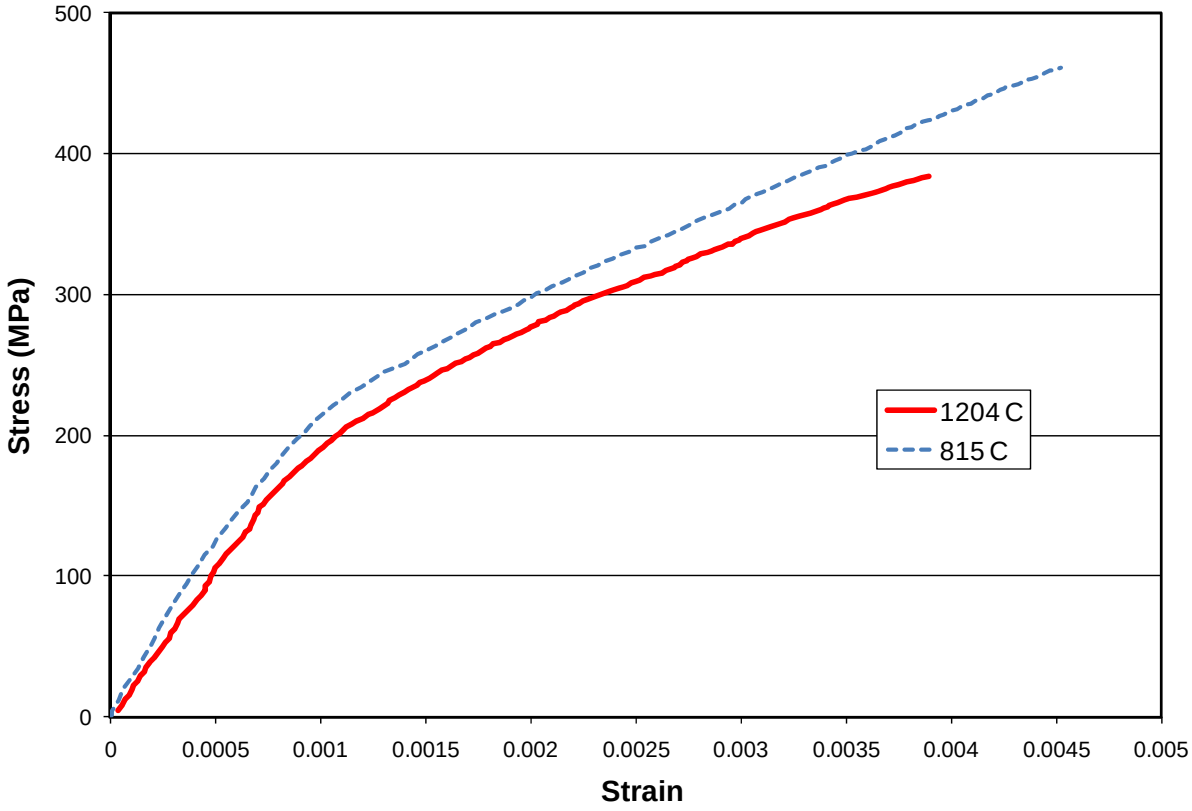

Figure 1: Stress-strain curves for specimens without holes at 815 and 1204 ^{o}C

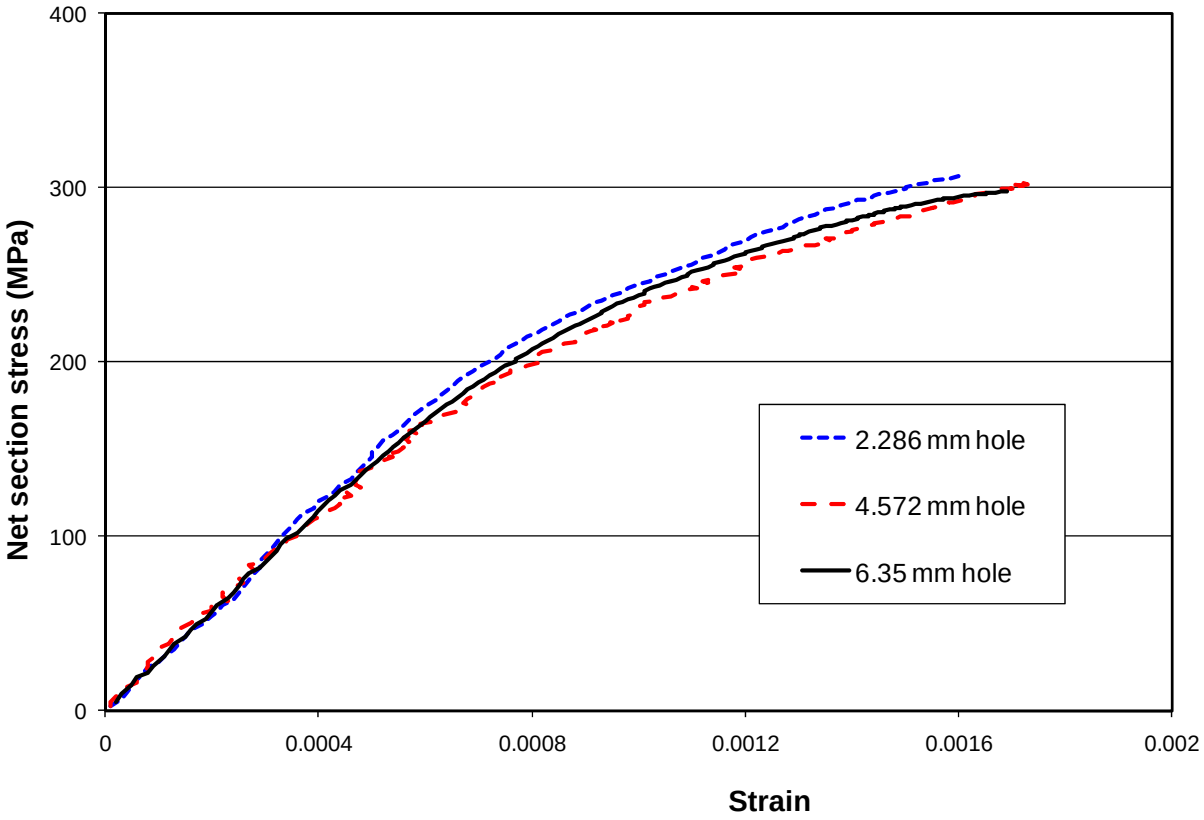

Figure 2: stress-strain curve for specimens with holes at 1204 ^{o}C

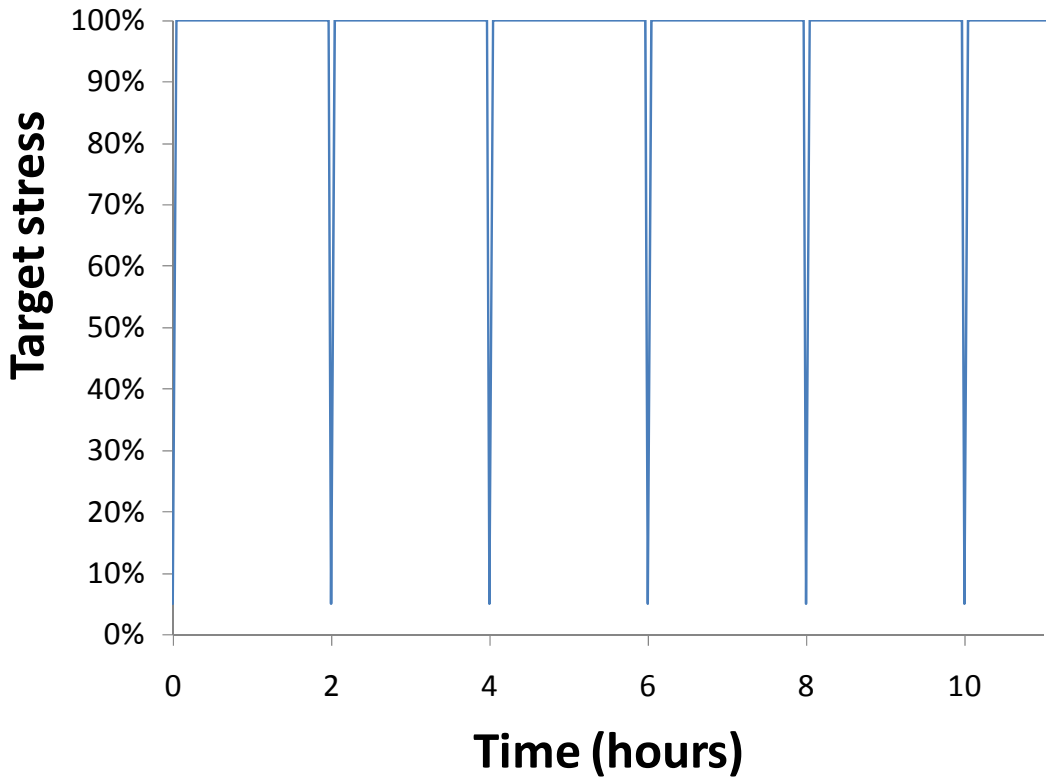

Figure 3: Stress-time profile for dwell-fatigue experiments

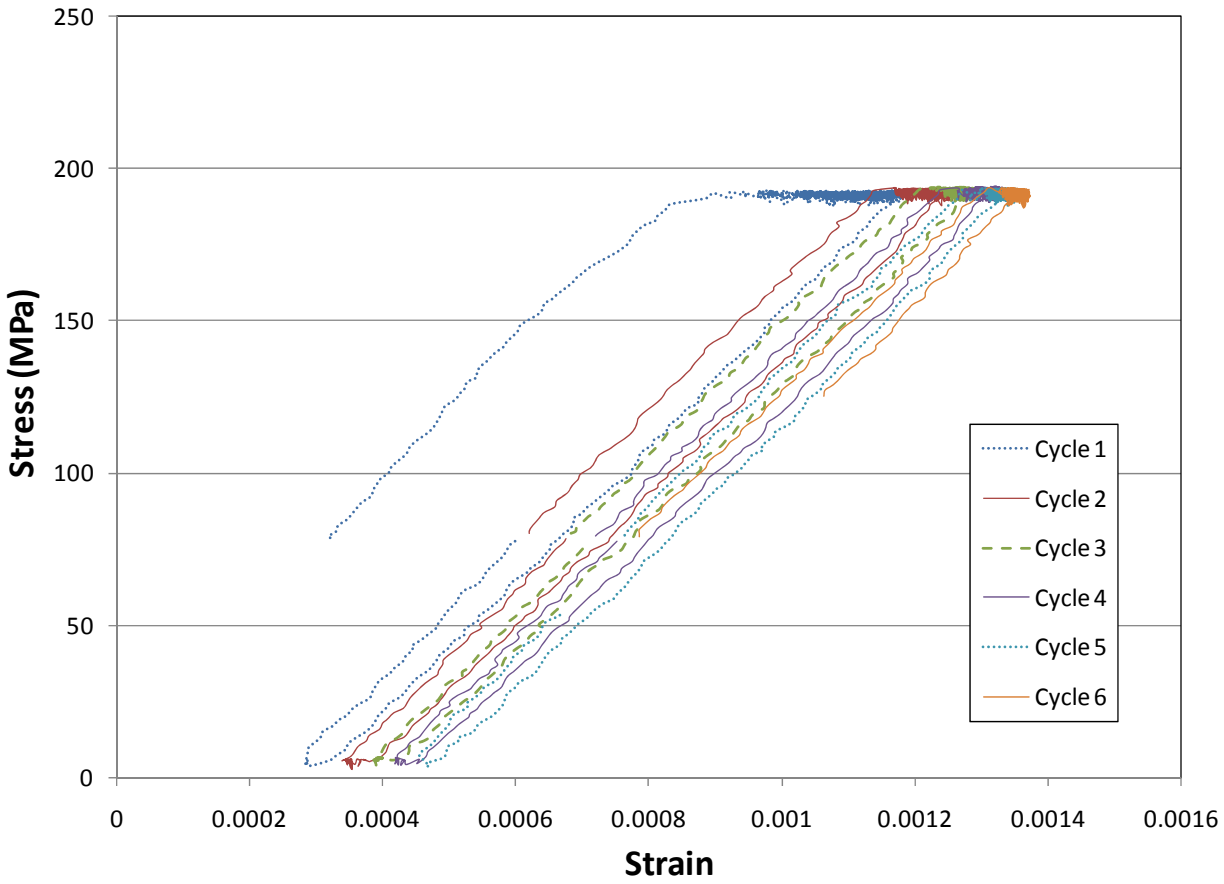

Figure 4: Typical stress-strain response for a dwell-fatigue experiment. Data shown is from the first six cycles of a 193.2 MPa test for a specimen without a hole at 1204 ^{o}C.

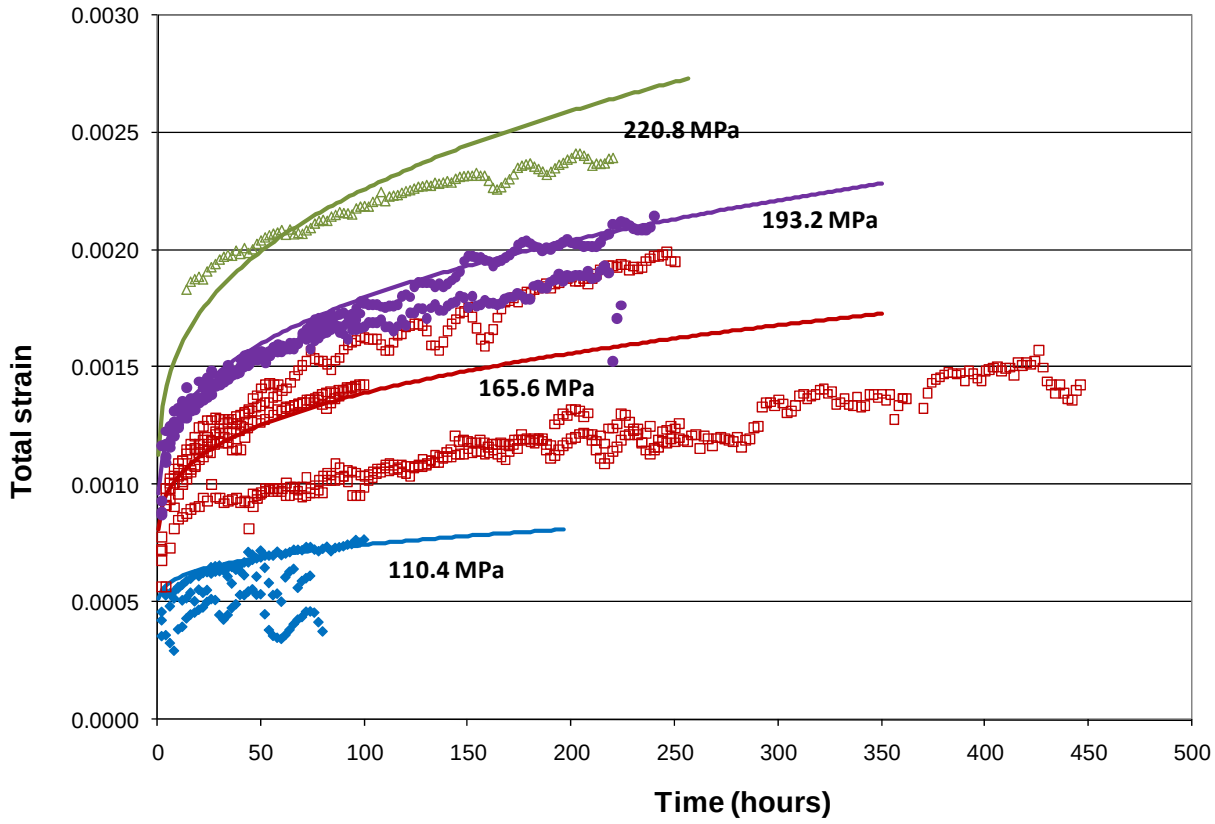

Figure 5: Total strain versus time response in dwell fatigue experiments for specimens without holes at various stress levels at 1204 ^{o}C. Experimental data points are marked in symbols, while solid lines indicate curve fitting using a 3-parameter equation.

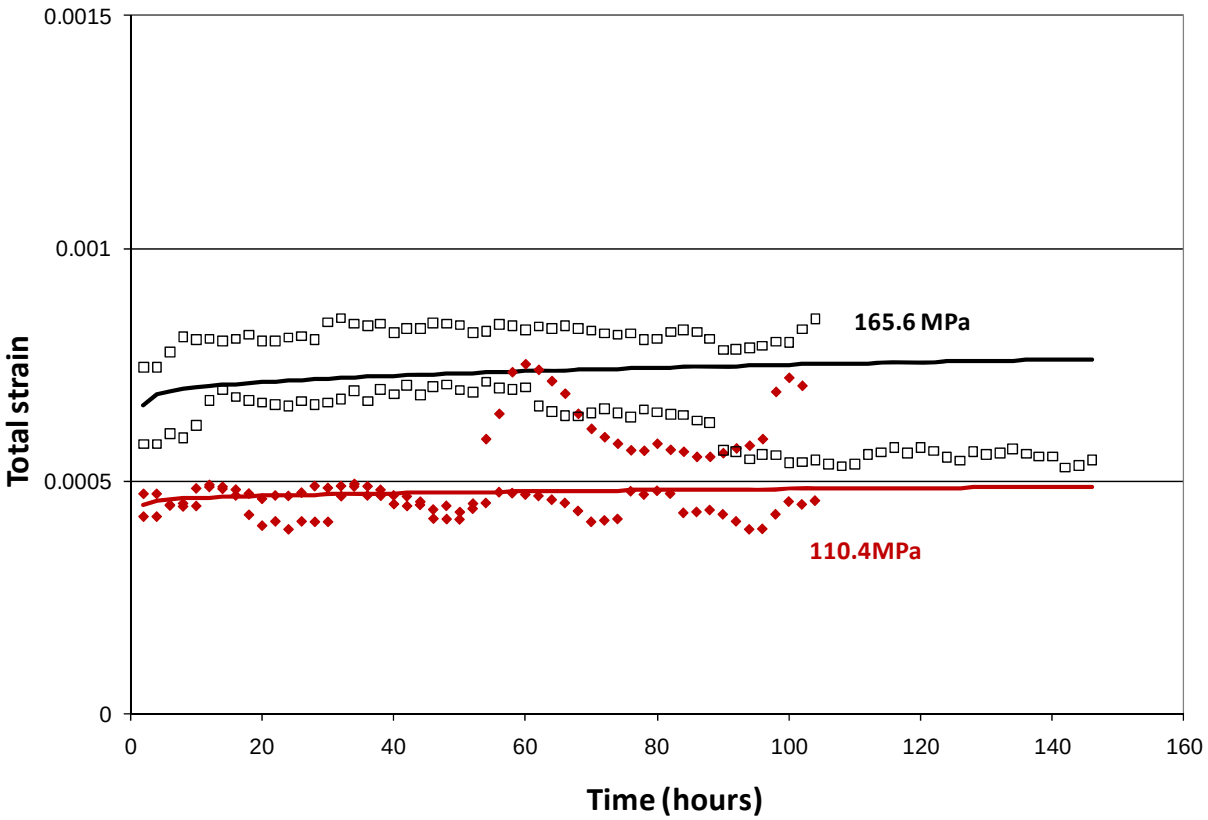

Figure 6: Total strain versus time response in dwell fatigue experiments for specimens without holes at 110.4 and 165.6 MPa at 815 ^{o}C. Experimental data points are marked in symbols, while solid lines indicate curve fitting using a 3-parameter equation.

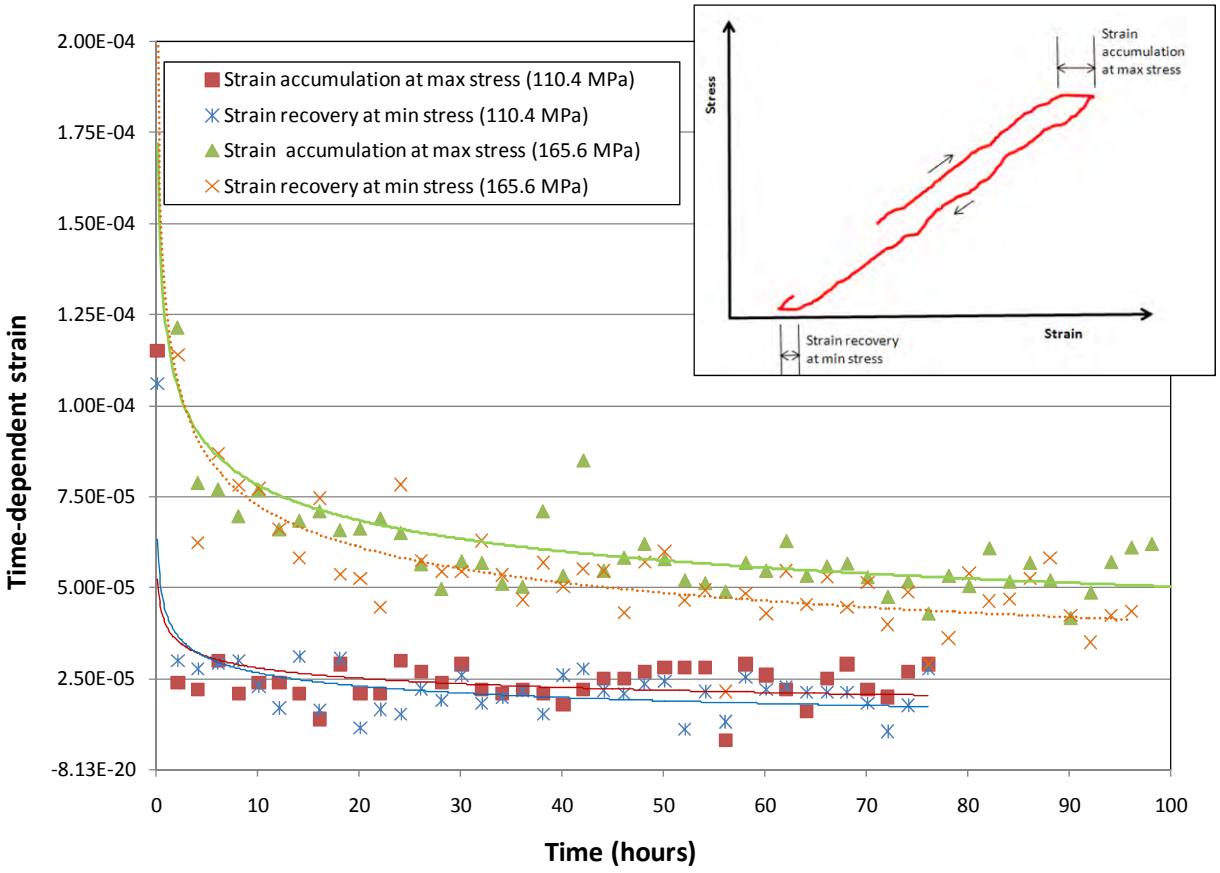

Figure 7: Strain accumulation at maximum stress and strain recovery at minimum stress versus time for specimens without holes loaded at stresses of 110.4 MPa and 165.6 MPa. Experimental data points are marked in symbols, while solid lines indicate curve fitting using a 2-parameter equation.

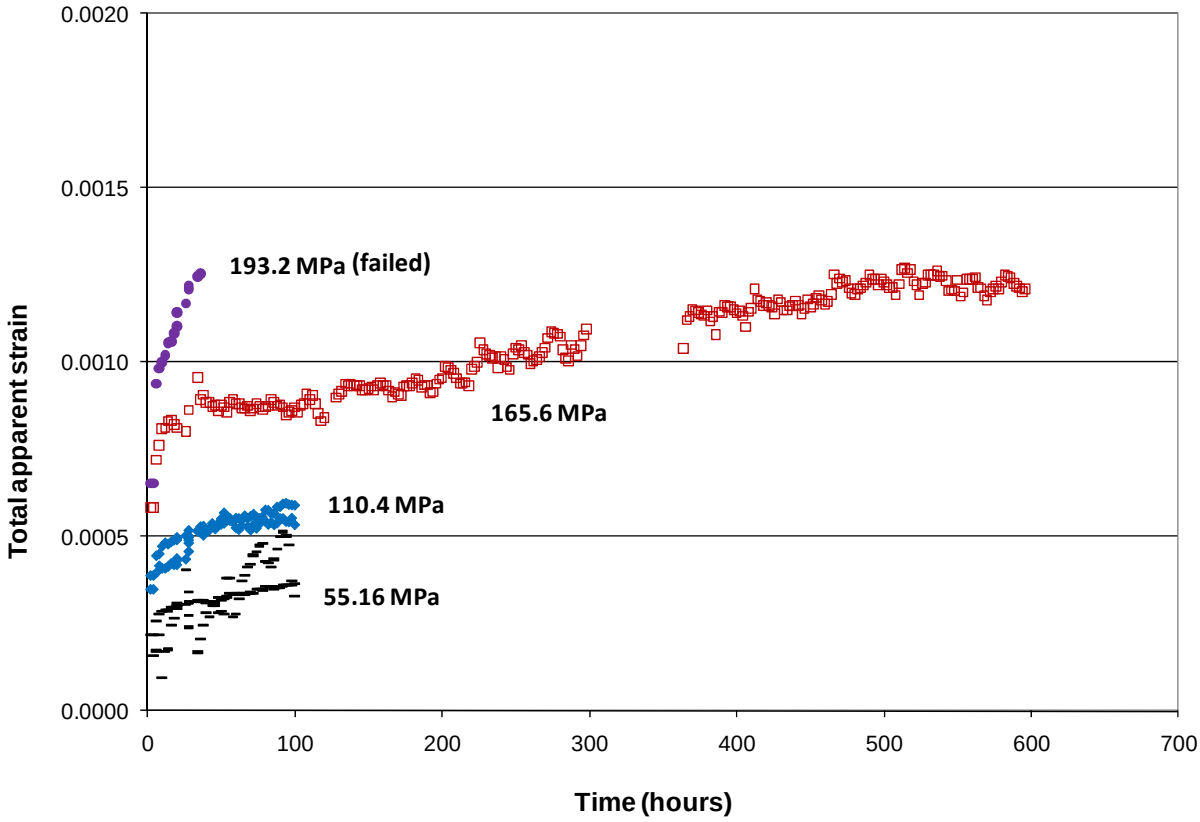

Figure 8: Total apparent strain versus time response in dwell fatigue experiments for specimens with a 2.286 mm central hole subjected to 55.16, 110.4, 165.6 and 193.2 MPa net-section stresses at 1204 ^{o}C.

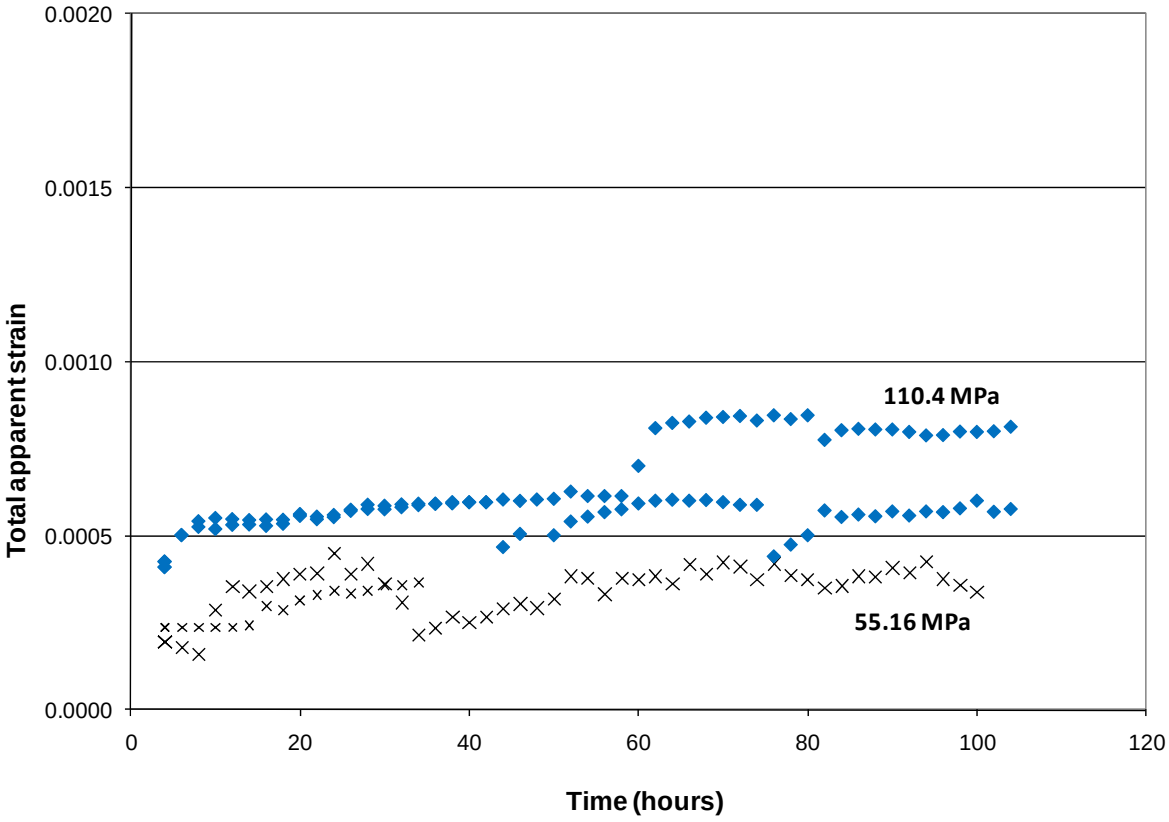

Figure 9: Total apparent strain versus time response in dwell fatigue experiments for specimens with a 4.572 mm central hole subjected to 55.16 and 110.4 MPa net-section stresses at 1204 ^{o}C.

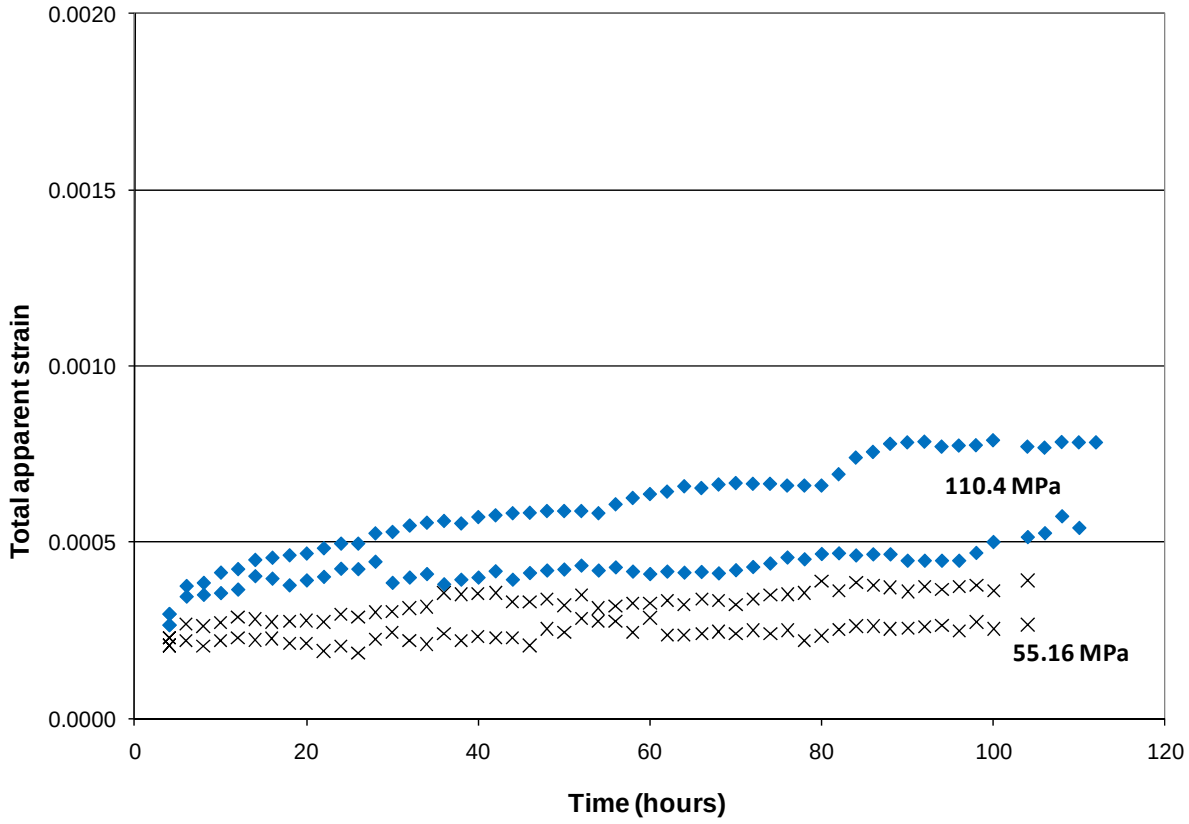

Figure 10: Total apparent strain versus time response in dwell fatigue experiments for specimens with a 6.35 mm central hole subjected to 55.16 and 110.4 MPa net-section stresses at 1204 ^{o}C.

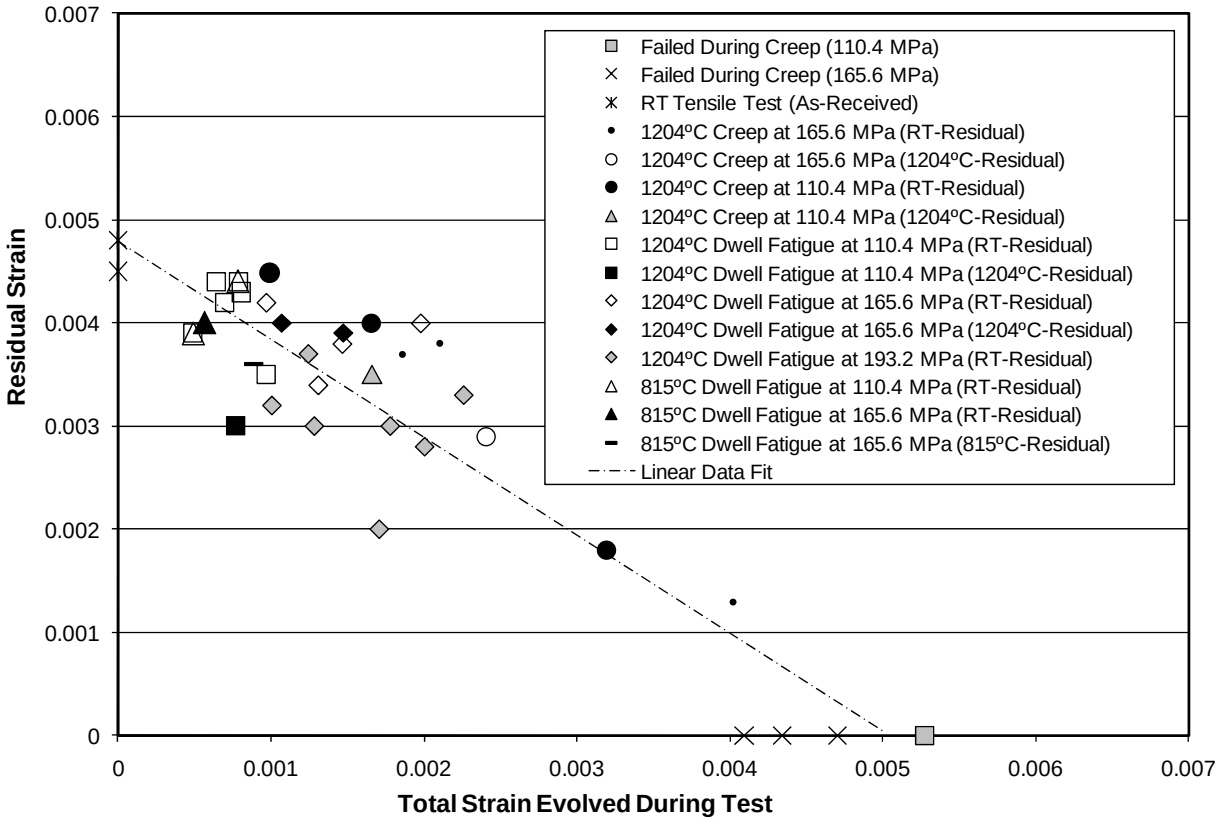

Figure 11: Residual strain to failure versus time-dependent strain during dwell fatigue experiments for specimens without holes tested at different stress levels. Experimental data points are marked by a solid circle and the solid line is curve fitting using a linear operator.

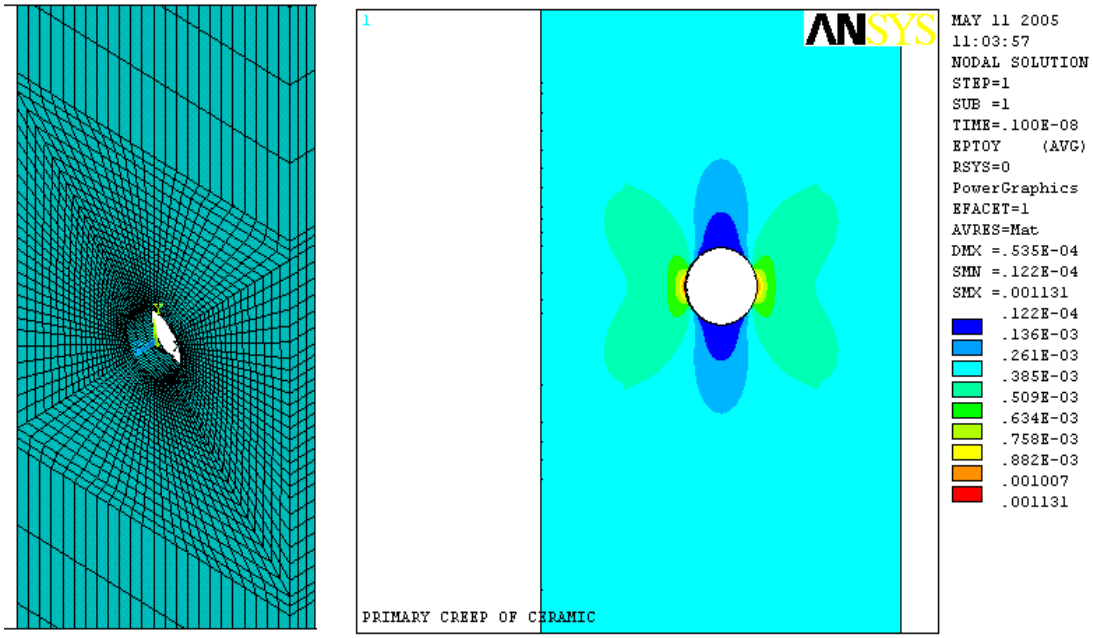

Figure 12: 3D meshing of specimen with a central hole (left), and the time-dependent strain accumulation under load in the area around the hole (right).

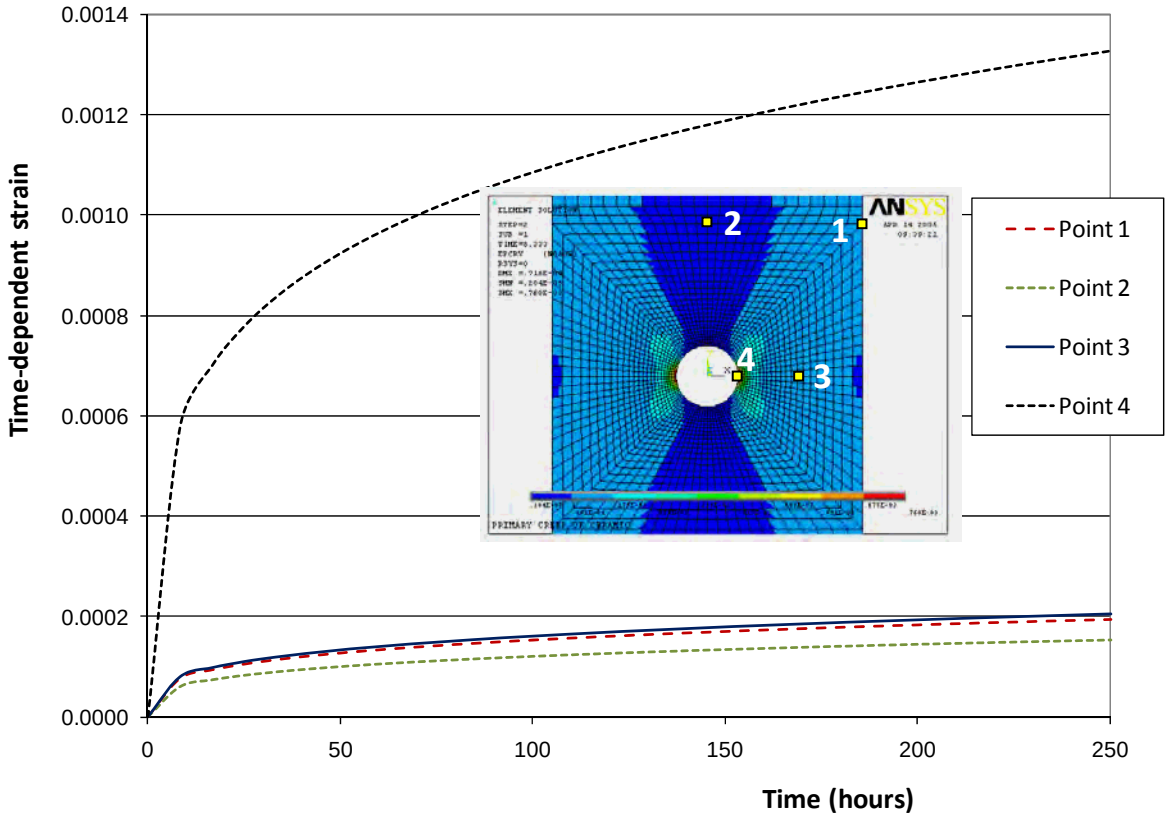

Figure 13: Total strain versus time at four different locations around a 4.572 mm central hole under a stress of 55.16 MPa at 1204 ^{o}C. The extensometer legs rested at point 1 providing the readings shown in Figure 9.

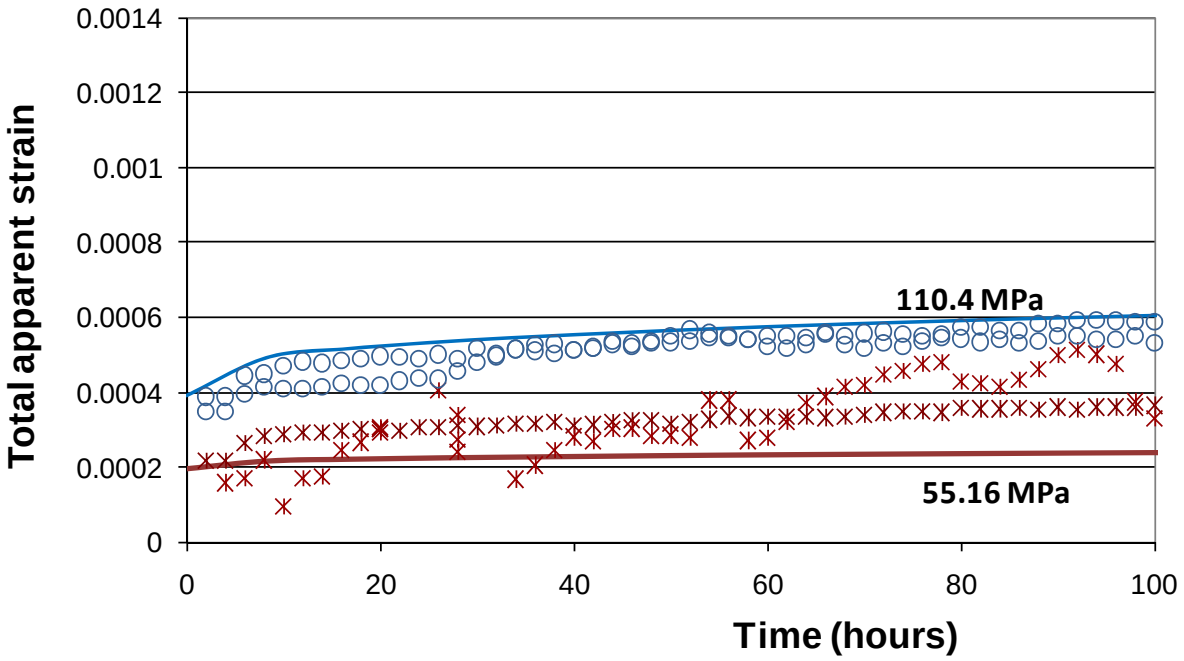

Figure 14: Experimental data and ANSYS® results for total strain versus time at point 1 for specimens with 2.286 mm central hole under a stress of 55.16 and 110.4 MPa tested at 1204 ^{o}C. Experimental data points are marked in symbols, while solid lines indicate result of ANSYS® runs.

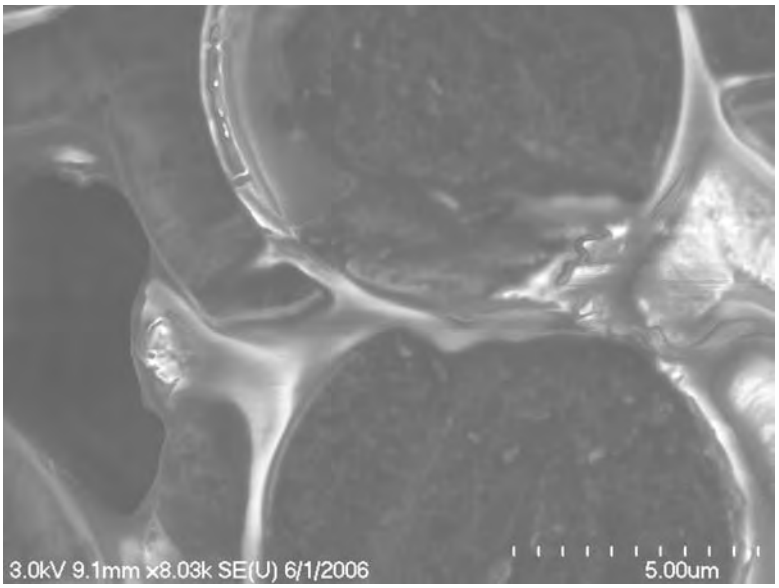

Figure 15: Oxidation of BN and flow of the glass phase around fibers. Image acquired after residual strength experiment from the failure region of a specimen without holes tested at a stress of 220 MPa in dwell fatigue.